40. ROCK-AND PALEOMAGNETISM OF DEEP SEA DRILLING PROJECT LEG 54 BASALTS — EAST PACIFIC RISE AND GALAPAGOS RIFT

N. Petersen, Institut für Allgemeine und Angewandte Geophysik,
Ludwig-Maximilians-Universität, Munich, West Germany
and
W. M. Roggenthen, Department of Geology and Geological Engineering,
South Dakota School of Mines and Technology, Rapid City, South Dakota

INTRODUCTION

The samples investigated in this study came from the following two areas:

a) The western slope of the East Pacific Rise (EPR) at about 9° N (Holes 420, 421, 422, 423, 427, 428, 428 A, and 429 A). The drill sites form a transect perpendicular to the EPR (see Figure 1). Only Site 427 is off this transect, about 100 km to the south, drilled in a deep trough in the Siqueiros fracture zone. The samples cover an age span from about 1.5 m.y. to 4.6 m.y.; all come from the Pacific plate. The EPR has a spreading rate of about 5.7 cm/y. at the latitude of the transect (this value has been obtained from an interpretation of the magnetic profile recorded during Leg 54, perpendicular to the EPR).

b) The area at the Galapagos spreading center at 86° W (Holes 424, 424 A, B, and C, and 425). Sites 424 and 425 are located (Figure 1) on opposite sides of the spreading axis: Site 424 to the south of it on the Nasca plate drilled into an area of geothermal activity (about 0.7 m.y. old) and Site 425 north of the axis on the Cocos plate (about 1.8 m.y. old), in an area of high heat flow (about 5 HFU). The spreading rate at this longitude is 3.25 cm/y. (Sclater and Klitgord 1973).

Both areas are situated very close to the equator, and a paleomagnetic correlation between the polarity of remanent magnetization of the drill cores and the sign of the overlying marine magnetic anomaly has therefore not been attempted. The samples are oriented only with respect to the vertical, which means that only the magnetization inclination can be determined. In the Galapagos area the Earth's magnetic field is nearly horizontal, and the sense of magnetization polarity of the drill cores cannot be measured (so it is not possible to tell if a sample is reversely or normally magnetized). At the latitude of the EPR holes the inclination of an Earth-centered dipole field is only 18° which is too shallow to give reliable results, since the secular variation of the Earth's magnetic field may easily exceed this value. In this study, therefore, we have emphasized rock magnetic investigations; in particular, the effect of submarine alteration of the magnetic mineral component has been investigated.

MAGNETIC AGES OF THE DRILL SITES

We have measured the total magnetic field intensity along profiles across the EPR and the Galapagos spreading center, perpendicular to the respective ridge axes and connecting the different drill sites. The individual marine magnetic anomalies could easily be identified (Figures 2 and 3), and so the different drill sites could be dated using the polarity time scale of Maniken and Dalrymple (1979). The ages thus obtained are listed in Table 1. Site 427 (Siqueiros fracture zone) could not be dated this way, as no magnetic profile was available for the area. The drilling site is located on the southern portion of the fracture zone and may belong to the block of oceanic crust to the south. If this assumption is true, an age estimate of this site can be made from its distance from the ridge crest. Assuming the same spreading rate as north of the Siqueiros fracture zone (5.7 cm/y), an age of 3.4 m.y. is calculated for Site 427. However, this age is probably too high, as will be shown in a later section. From studies of the degree of alteration of the magnetic minerals, an age of about 2 m.y. is deduced.

PALEOMAGNETIC MEASUREMENTS

Instruments and Methods

The natural remanent magnetization (NRM) of the rocks was measured onboard ship using a Digico spinner magnetometer. Alternating field demagnetization was carried out on board with a Schonstedt single-axis demagnetizing unit. Additional magnetic measurements were made at the University of Munich, also with a Digico spinner magnetometer, and with a two-axis tumbling AF-demagnetizing unit. The stepwise alternating field demagnetization was carried out with 25, 50, 75, 100, 150, 200, 300, 400, 500, and 1000 Oe in a field-free space in order to determine the "stable direction" of magnetization. Volume susceptibility was measured with a Bison magnetic susceptibility bridge.

The magnetic stability was characterized by the median destructive field (MDF), which is the peak alternating field necessary to erase half of the NRM. The coarser grained rocks often had a rather unstable rema-
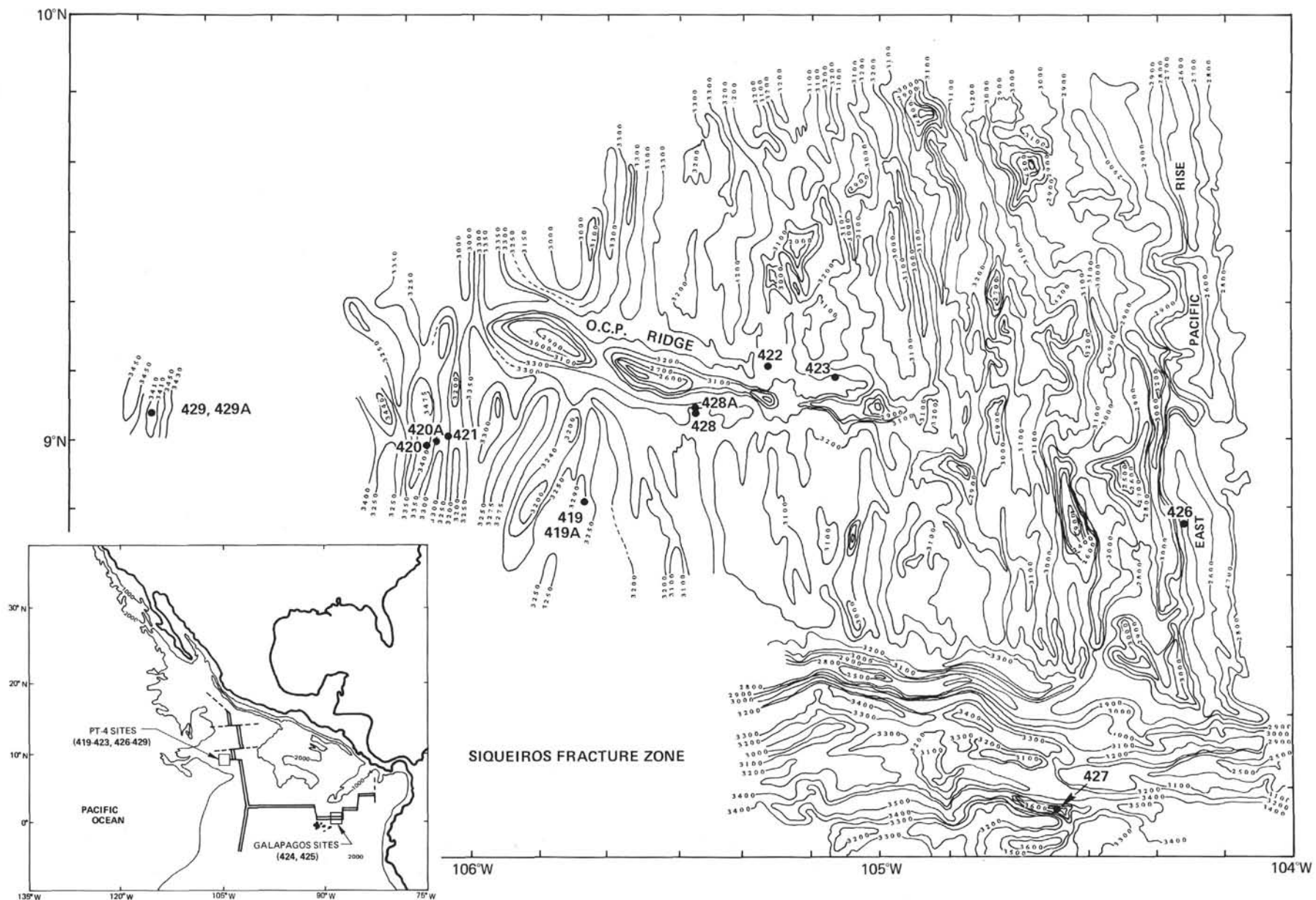
Figure 1. *Locations of sites drilled on Deep Sea Drilling Project Leg 54.*
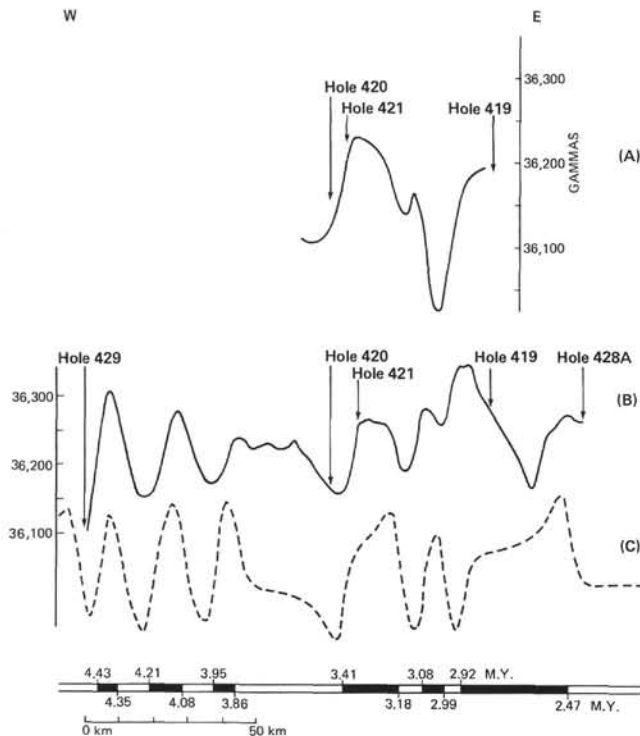
Figure 2. *(A) Magnetic profile generated during cruising west from Site 419. (B) Magnetic profile due west of Hole 428A. Sites 420 and 421 have been projected into two profiles. (C) Model anomaly pattern created by assuming blocks to be bearing 10°E and 1 km thick. Ages of anomalies are from Maniken and Dalrymple (1979) modified after the magnetic polarity time scale of LaBrecque et al. (1977).*

Figure 3. *(A) Observed profile over the Galapagos Ridge showing the locations of Sites 424 and 425. (B) Model profile generated from 1-km-thick magnetized crust. Ages of anomalies are from Maniken and Dalrymple (1979).*

TABLE 1
Magnetic Ages of the Drill Sites

East Pacific Rise

Site	Age (m.y.)
420	3.4
421	3.4
422	1.7
423	1.5
427	2.0[a]
428	2.4
429	4.6

Galapagos

Site	
424	0.7
425	2.0

[a]Site 427 has been dated from the degree of alteration of the titanomagnetites.

nent magnetization and relatively large viscous components. In such cases the "stable direction" of magnetization could not be determined with certainty. In Table 2a and b these samples are marked with "?."

Results

The data are summarized in Table 2a and b. Figure 4 shows the downhole plot of NRM intensity, stable remanence direction, and Curie temperature (T_c) for Hole 428 A, which is the hole with the deepest crustal penetration reached during Leg 54. As described later in the section on rock magnetism, the Curie temperature of the completely unaltered rock is only 125° C. The dashed line in Figure 4 represents this value for comparison. It can be seen that none of the Hole 428 A samples has retained this original value. The increase of Curie temperature is most likely caused by submarine low-temperature oxidation (Ozima et al., 1974; Prévot and Lacaille, 1976; Bleil and Petersen, 1977; Johnson and Hall 1978; Petersen et al., in press) and will be subsequently discussed in more detail.

Hole 428 A was drilled well within the Matuyama reversed magnetic field epoch. From Figure 4 it can be seen that the magnetization polarity of the drilled samples agrees well with the negative sign of the overlying marine magnetic anomaly. However, as already pointed out, this could be fortuitous since it may be caused by the secular variation of the Earth's magnetic field.

The effect of secular variation of the Earth's magnetic field can be recognized in Figure 5, which shows a downhole plot of the remanence directions for Hole 424. Zero inclination would be expected theoretically at this site, almost directly at the equator. On the other hand, the observed deviation from zero inclination in Figure 4 could be due to tilting of a portion of the oceanic crust around an axis parallel to the ridge. However, this seems less likely, as we would then expect either a constant deviation or one increasing with depth.
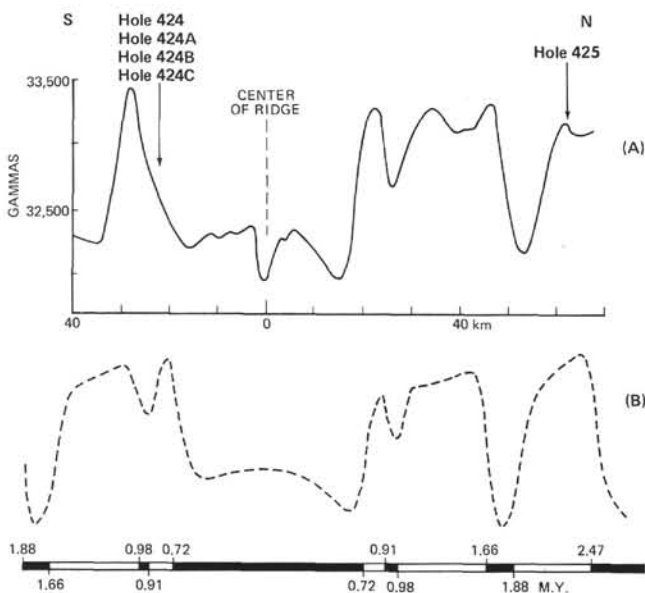
TABLE 2a
Compilation of Different Magnetic Parameters of All Measured Samples From the East Pacific Rise Boreholes

Sample Core-Section, Interval in cm, Piece No.	NRM Intensity $(10^{-3}$ Gauss)	NRM Inclination (°)	Stable Inclination[a] (°)	Susceptibility $(10^{-4}$ Gauss/Oe)	Q-factor[b]	MDF[c] (Oe)	Curie Temperature (°C)	I_s[d] $(10^{-2}$ Gauss cm/g)
Hole 420								
13, CC, 53-56	1.977	+12.5?	+13.5?	1.36	40	610	282	16
14-1, 14-17	1.020	−20.4	−19.5	1.20	24	720	−	−
15-1, 70-72, 9	7.943	+15.6?	+16?	1.43	154	530	−	−
17-1, 27-30	9.996	−	−	−	−	960	−	−
Hole 421								
3-1, 30-33, 5	0.867	−5.8	−6	1.6	15	840	−	−
3-1, 72-75	1.079	−14.7	−15	1.76	15	950	270	15
3-1, 117-120, 17	1.489	−40.5	−42	0.93	44	790	−	−
4-1, 4-7, 1	1.059	−49.1	−49	0.84	35	860	−	−
bit, 10-13, 2	1.544	−58.7	−57.5	1.6	27	930	−	−
Hole 422								
7-1, 39-42, 6A	1.272	−14.8	−9	22.7	1.6	20	−	−
7-1, 45-48, 6B	4.029	−46.1	−21	−	−	60	110	73
7-1, 89-92, 7E	3.446	−31.9	−9?	19.9	5	45	−	−
7-2, 14-17, 3	4.329	−34.2	−17	20.4	6	50	110	68
8-5, 23-26, 5	3.196	−47.6	−9?	15.7	6	<100	−·	−
8-5, 127-130, 14	3.573	−38.2	−20	−	−	40	120	76
8-5, 132-135, 14	5.685	−40.8	−13?	22.4	7	45	−	−
9-1, 38-41, 4A	4.056	−42.7	−17.5	−	−	63	120	72
9-1, 70-73, 4C	3.259	−37.8	−20	23.8	4	40	−	−
9-2, 19-22, 3	2.540	−46.7	−23?	−	−	62	150	84
9-2, 45-48, 4B	3.323	−46.6	−24	20.8	4	85	−	−
9-2, 135-138, 6A	4.235	−42.5	−30	16.6	7	75	−	−
9-3, 23-26, 4A	4.007	−47.3	−36	−	−	30	180	65
9-3, 91-94, 6C	3.930	−34.4	−28	18.4	6	85	−	−
9-4, 10-13, 1	3.018	−47.9	−27	−	−	70	180	66
9-4, 135-138, 13A	6.386	−27.8	−23	15.7	11	80	−	−
9-4, 143-146, 13B	5.156	−26.3	−13	−	−	78	230	63
9-5, 31-34, 3B	−	−	−	−	−	−	213	63
9-5, 72-76, 6	2.587	−31.2	−25	16.5	4	75	−	−
Hole 423								
5, CC	0.885	−28.2	−27	1.1	23	1080	−	−
7-1, 4-7, 1	0.401	−73.8	−67	1.1	11	1000	241	8
Hole 427								
9-1, 11-13, 2	9.184	−39.1	−17	29	9	197	−	−
9-1, 25-27, 3	9.211	−34.6	−13	−	−	175	225(485)	159
9-1, 41-44, 4B	5.111	−42.7	−20	41	3.5	110	−	−
9-1, 84-87, 8	10.721	−30.2	−20	−	−	110	215	150
9-1, 103-106, 10	10.317	−32.2	−16	32	9	118	−	−
9-2, 4-7, 1	7.063	−47.9	−23	46	4	68	−	−
9-2, 64-67, 8	4.863	−45.7	−25?	47	3	65	160	145
9-2, 94-97, 11A	4.199	−63.7	−32	50	2.3	52	−	−
9-2, 129-132, 13	4.907	−45.0	−31	45	3	67	155	139
9-3, 4-7, 1	10.692	−18.1	−13	30	10	133	205(480)	160
9-3, 56-59, 5A	10.576	−25.5	?	−	−	25	240(465)	169
9-3, 62-65, 5B	6.556	−39.8	−25	41	4	77	−	−
9-3, 137-140, 9	4.231	−72.6	?	44	3	63	210	149
9-4, 36-39, 4A	3.596	−55.9	−20?	53	2	45	−	−
9-4, 132-135, 6	5.063	−77.6	−17?	47	3	55	−	−
9-5, 96-99, 7	4.128	−63.3	−20	58	2	45	−	−
9-5, 107-110, 7	−	−	−	−	−	−	130	144
10-1, 67-70, 4A	4.806	−78.8	−47?	55	2.4	45	−	−
10-1, 118-121, 6A	−	−	−	−	−	−	130	137
10-2, 5-8, 1A	5.660	−64.2	−34?	54	3	37	−	−
10-2, 131-134, 4	5.522	−77.6	−36?	51	3	42	−	−
10-3, 39-42, 3	4.796	−78.8	−27	50	2.7	45	−	−
10-3, 109-112, 9A	1.962	−41.6	−12?	−	−	77	200	148
10-3, 144-147, 9C	3.425	−53.9	−36	42	2.3	65	−	−
10-4, 33-35, 1D	4.813	−55.1	?	36	4	78	245	145

TABLE 2a – *Continued*

Sample Core-Section, Interval in cm, Piece No.	NRM Intensity (10^{-3} Gauss)	Inclination (°)	Stable Inclination[a] (°)	Susceptibility (10^{-4} Gauss/Oe)	Q-factor[b]	MDF[c] (Oe)	Curie Temperature (°C)	I_s[d] (10^{-2} Gauss cm/g)
Hole 427								
10-4, 74-77, 1G	4.842	−47.3	−16	31	4	91	−	−
10-4, 123-126, 1J	−	−	−	−	−	−	265	144
10-4, 143-146, 1K	6.439	−39.7	−12	28	6	120	255	142
10-5, 64-67, 4B	5.035	−42.7	−15	41	3	91	−	−
10-5, 106-109, 7	−	−	−	−	−	−	180	140
Hole 428								
5-4, 15-18, 2	2.924	+47.6	+42?	14	6	195	−	−
5-4, 36-39, 4	6.456	−30.4	−22	23	8	92	−	−
5-4, 72-75, 8	9.033	+24.5	−17.5	18	14	65	−	−
5-4, 81-84, 9	4.719	−26.7	−19	26	5	80	−	−
6-1, 18-21, 3	7.354	−31.2	−20	22	9	65	−	−
6-1, 74-77, 8C	7.584	−46.1	−22	24	9	58	148	91
6-1, 127-130, 10B	6.362	−46.2	−19	15	12	75	−	−
6-2, 6-9, 1	9.130	−46.9	−22?	29	9	47	−	−
6-2, 75-78, 8	5.822	−36.8	−24	28	6	55	−	−
Hole 428A								
1-1, 32-35, 4	7.394	−53.6	−32	27	8	98	217	116
1-1, 89-92, 10	8.526	−43.6	−26	24	10	75	−	−
1-2, 4-7, 1	8.740	−37.1	−24	12	20	130	−	−
1-2, 47-50, 6	4.835	−54.1	−31	18	7	62	−	−
1-2, 125-128, 13B	7.897	−47.3	−34	23	6	80	−	−
1-3, 65-68, 3B	5.564	−57.7	−31	26	6	60	−	−
1-3, 79-82, 3C	6.077	−51.4	−33	−	−	60	155	104
1-4, 5-8, 1	4.662	−55.5	−35	25	5	74	−	−
1-4, 72-78, 9	7.967	−38.2	−19	19	12	90	−	−
2-1, 20-23, 3	6.266	−65.4	−26	18	10	84	−	−
2-1, 25-28, 4	5.659	−76.3	−26	18	9	80	−	−
2-1, 68-71, 8	8.876	−34.1	−21	−	−	85	177	73
2-1, 77-80, 8	8.844	−37.6	−19	17	14	83	−	−
3-1, 27-30, 5	0.630	−	−	1	17	590	−	−
3-1, 76-79, 10A	3.060	−39.5	−24	−	−	33	160	110
3-1, 112-115, 8	3.681	−43.9	−35	31	3	75	−	−
3-1, 134-137, 12A	6.030	−26.5	−23	28	6	105	−	−
4-1, 50-53, 9A	5.484	−28.3	−23	20	8	197	−	−
4-1, 114-117, 14	4.274	−35.6	−29	21	6	160	−	−
4-2, 3-6, 1	7.861	−33.4	−26	22	10	175	−	−
4-2, 76-79, 6A	4.115	−22.0	−31?	−	−	95	225	115
4-2, 118-121, 8	5.613	−34.6	−27	4	39	93	−	−
4-3, 57-60, 5	5.241	+63.7	−25	34	4	20	−	−
5-1, 21-24, 3A	4.456	−42.7	−30	28	4	87	−	−
5-1, 115-118, 9	4.337	−40.4	−27	32	4	85	−	−
5-2, 12-15, 1A	2.863	−36.4	−27?	36	2	63	−	−
5-2, 85-88, 5D	−	−	−	−	−	−	160	110
5-2, 93-95, 5E	3.128	−50.8	−31?	37	2	43	−	−
5-2, 114-117, 6	3.854	−39.5	−23	9	12	155	245	89
5-3, 31-34, 3	3.507	−55.9	−30?	32	3	70	−	−
5-3, 85-88, 9	3.696	−45.8	−21	−	−	130	175	102
5-3, 123-126, 12	6.162	−47.6	−29	30	6	70	−	−
5-4, 10-13, 1	3.964	−39.9	−17?	−	−	92	170	104
5-4, 89-92, 6	5.547	−49.3	−19	31	5	65	153	102
6-1, 38-41, 6	4.024	−	−	−	−	145	190	95
6-1, 52-55, 8	7.036	−47.3	−21	24	8	90	176	104
6-1, 75-78, 11	3.888	−20.5	−23	−	−	95	−	−
6-1, 100-103, 13	4.388	−37.7	−23	22	6	70	−	−
7-1, 15-18, 2	5.162	−37.8	−20	21	7	112	−	−
7-1, 39-42, 4	8.291	−28.3	−15	−	−	122	230(495)	110
7-1, 88-91, 6E	3.984	−83.1	−33?	31	4	64	−	−
7-2, 6-9, 1A	4.976	−83.6	−25?	34	4	47	−	−
7-2, 87-89, 6	−	−	−	−	−	−	270	63
7-2, 147-150, 12	5.700	−49.7	−24	20	8	50	−	−

TABLE 2a – *Continued*

Sample Core-Section Interval in cm, Piece No.	NRM Intensity (10^{-3} Gauss)	Inclination (°)	Stable Inclination[a] (°)	Susceptibility (10^{-4} Gauss/Oe)	Q-factor[b]	MDF[c] (Oe)	Curie Temperature (°C)	I_s[d] (10^{-2} Gauss cm/g)
Hole 429A								
1-1, 60-63, 3	1.275	+22.9	+30	3	12	255	–	–
2-1, 15-18, 3	1.333	+29.9	+30	2	18	720	330	15
2-1, 26-29, 4	1.509	+28.1	+29	2	21	295	–	–
2-1, 41-44, 5B	1.443	+25.9	+28	2	20	355	–	–
2-1, 53-56, 7	1.149	−75.7?	−75?	2	16	315	–	–
2-1, 87-90, 12	0.721	−16.9	−17	2	10	665	285	11
2-1, 125-128, 17	0.676	−17.4	−14	2	9	760	260	17
2-2, 10-13, 2	0.353	+10.0	+11?	1	10	920	–	–
3-1, 103-105, 5	5.333	−8.1	−6	35	4	75	87	82
3-1, 112-115, 6	3.865	−14.0	−5	29	4	90	–	–
3-1, 120-123, 7A	2.429	−45.9	−7	31	2	32	–	–

[a] Inclination of NRM after partial alternating field demagnetization.
[b] NRM/magnetization induced by the present Earth's magnetic field.
[c] MDF (median destructive field) is the magnetic field necessary to erase half of the NRM by alternating field demagnetization.
[d] I_s is the specific magnetization measured in 1800 Oe at room temperature.

Also for Hole 424, we have observed Curie temperatures slightly higher than those of a completely unaltered rock.

ROCK MAGNETIC MEASUREMENTS

Instruments and Methods

a) Thermomagnetic Curves

Curie temperatures (T_c) and specific saturation magnetizations (I_s) were determined by measuring the temperature dependence of the strong field induced magnetization (thermomagnetic curve) with a Forrer-type automatically recording translation balance; the applied magnetic field was 1800 Oe. During the measurements the samples were kept in argon to reduce chemical alteration on heating. From the thermomagnetic curves, the Curie temperatures were determined by the graphical method of Grommé et al. (1969).

b) Microscopic Observations

The magnetic measurements were complemented by ore microscopic observations. Polished sections were studied under reflected light with a Leitz Ortholux Pol microscope. A magnetic colloid was used to aid the identification of magnetic minerals.

c) Microprobe Analyses

Microprobe studies of the magnetic minerals (titanomagnetites) were carried out on a number of samples from Hole 428A. A Geoscan (Cambridge Instruments) electron microprobe, equipped with two spectrometers, located at the Institute of Geology, University of Munich, was used. The titanomagnetite grains selected for the microprobe analyses had to be homogeneous and larger than 10 μm in diameter. The samples were prepared as polished sections and coated with a thin carbon layer. An acceleration voltage of 20 kV and a specimen current of 40 μA were used with a 20-s counting period.

All titanomagnetite grains were analyzed for Fe, Ti, Al, Mg, Mn, Cr, and Si. The last-mentioned element was measured to estimate the effect of the surrounding silicate matrix and to reject analyses giving excessive Si contents, assuming that titanomagnetite does not contain Si. Synthetic spinels were used as reference standards. The results are given as weight percentages of the elements instead of the usual oxide percentages, since oxygen cannot be measured with the microprobe used in this study.

Results

a) Microscopic Observations

The opaque minerals in the basalts investigated are predominantly titanomagnetites, members of the solid solution series $Fe_{3-x}Ti_xO_4$ ($0 \leq x \leq 1$). As will be discussed further, the range of compositions of the primary titanomagnetites in tholeiitic oceanic basalts in general, prior to any alteration, is very limited, with most x-values between 0.58 and 0.65. Titanomagnetite is the main carrier of remanent magnetization; the contribution of the other opaque minerals can be neglected. The titanomagnetite volume content of the samples investigated varies between 0.5 per cent and 3.0 per cent. A volume content of 1 per cent is typical for the fragmented basalts encountered in Holes 420, 421, 422, 423, and 429 A. The coarser grained basalts, particularly the samples from Holes 427 and 428A, have a higher titanomagnetite content of about 3 per cent, which is also expressed in the higher intensity of saturation magnetization (see Table 2a).

The titanomagnetite grains in all the samples studied here are skeletal. This is a typical feature in ocean-floor tholeiites (Petersen et al., in press). In the coarser grained samples, two fractions of titanomagnetite are observed: a fraction of grains up to 150 μm in size, usually skeletal to subhedral forms, and a fraction with skeletal to anhedral forms, 10 μm and smaller. Apart

TABLE 2b
Compilation of Different Magnetic Parameters of All Measured Samples from the Galapagos Spreading Center Boreholes

Sample Core-Section Interval in cm, Piece No.	NRM Intensity (10^{-3} Gauss)	NRM Inclination (°)	Stable Inclination[a] (°)	Susceptibility (10^{-4} Gauss/Oe)	Q-factor[b]	MDF[c] (Oe)	Curie Temperature (°C)	I_s[d] (10^{-2} Gauss cm/g)
Hole 424								
4-6, 113-116, 3	6.623	−54.2	+2	39	5	42	123	130
4-6, 139-143, 4C	−	−	−	−	−	−	132	133
5-1, 31-34, 5	12.969	−43.9	+4	26	14	82	−	−
5-1, 78-81, 9B	−	−	−	−	−	−	175	137
5-1, 126-129, 13	5.586	−42.5	−10	27	6	41	−	−
5-2, 118-121, 6	−	−	−	−	−	−	130	140
5-3, 22-25, 2	10.332	−62.3	+2	40	7	45	−	−
5-4, 10-13, 1	6.776	−63.0	−20?	47	4	40	121	135
6-1, 29-32, 5	3.666	−36.7	+14	42	2	90	−	−
6-1, 68-71, 8B	−	−	−	−	−	−	125	127
6-1, 107-110, 10C	11.414	−58.4	+5	34	9	40	−	−
6-2, 12-15, 1B	8.783	−64.4	−10	−	−	38	121	133
6-2, 32-35, 2A	6.541	−77.8	−5?	44	4	33	125	147
6-2, 113-116, 6C	−	−	−	−	−	−	142	147
6-3, 21-24, 1D	6.787	−58.3	+5	31	6	50	190	142
Hole 424A								
3, CC, 10-13, 1	10.369	−	−	13	22	120	163	87
Hole 424B								
5-1, 89-92, 12	10.139	−48.6	+9	27	10	55	150	117
5-1, 123-126. 16	−	−	−	−	−	−	198	94
5-1, 139-141, 17	10.620	−29.3	+8.5	28	10	60	−	−
5-2, 15-18, 2	7.240	−26.9	+18	33	6	40	125	117
5-2, 53-56, 6	12.379	−	−	20	17	55	137	107
6-1, 65-68, 10	13.263	−42.3	−16	21	17	70	−	−
6-1, 65-68, 10	9.896	−60.9	−11	26	11	47	−	−
Hole 424C								
3-1, 20-23, 2	7.157	−39.2	+23	26	8	45	133	120
3-1, 37-40, 3	15.374	−14.7	+18	−	−	60	150	111
3-1, 46-49, 4	11.428	+7.2	+23	8	41	155	−	−
Hole 425								
7-1, 25-28, 5	4.350	−17.8	−4?	−	−	125	262(495)	53
7-1, 45-48, 7	6.798	−22.8	+16	25	8	76	160	113
7-1, 67-70, 9	3.530	−64.1	−4?	−	−	120	155	107
7-1, 90-93, 12	19.977	+12.6	+30	17	33	105	197	101
7-1, 130-133, 17	11.647	+8.3	+23	21	15	76	−	−
7-2, 34-37, 4	3.263	−12.0	+25	27	3	47	157	102
7-2, 60-63, 7B	1.942	−63.0	+25	28	2	35	−	−
7-2, 115-118, 11	1.718	−39.0	+37	27	2	47	−	−
8-1, 44-47, 6	2.193	−39.6	+29	21	3	63	175	102
8-1, 70-73, 9	2.267	−51.3	+20	31	2	37	−	−
8-1, 80-83, 10	2.182	−50.7	+10	30	2	38	−	−
8-1, 93-96, 11	9.482	−9.9	−3	22	12	90	−	−
8-1, 145-148, 16	6.059	−39.9	−3	20	8	66	−	−
9-1, 26-29, 5	4.518	−38.0	−8?	28	4	45	160	102
9-1, 125-128, 17	5.108	−42.5	−12	26	5	58	210	93
9-2, 34-37, 4	−	−	−	−	−	−	215	93
9-2, 42-45, 4	4.514	−40.5	−12	20	6	84	−	−
9-2, 67-69, 7	6.857	−34.7	−19	24	8	95	215	90
9-2, 102-105, 11	6.045	−36.7	−22?	−	−	132	315	100
9-2, 120-122, 13	7.062	+11.9?	+2?	17	11	150	−	−
9-2, 129-131, 14	1.349	−	−	29	13	56	−	−
9-2, 134-137, 15	−	−	−	−	−	−	190	98
9-3, 69-72, 10	3.016	−57.8	−17	22	4	55	−	−

[a] Inclination of NRM after partial alternating field demagnetization.
[b] NRM/magnetization induced by the present Earth's magnetic field.
[c] MDF (median destructive field) is the magnetic field necessary to erase half of the NRM by alternating field demagnetization.
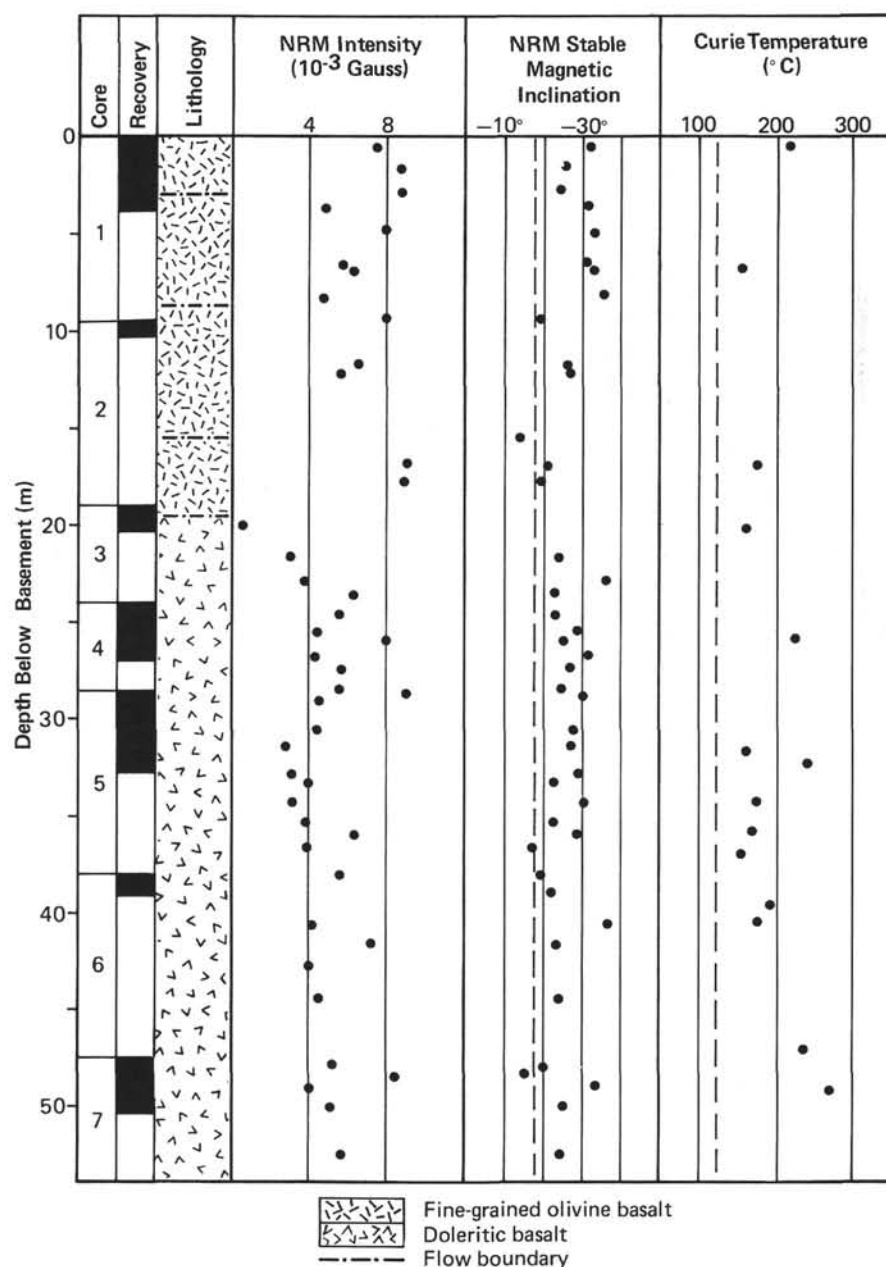[d] I_s is the specific magnetization measured in 1800 Oe at room temperature.

Figure 4. *Downhole plot of intensity and direction of the natural remanent magnetization (NRM) and of Curie temperature for the East Pacific Rise Hole 428A. The depth of the individual samples has been calculated by assuming proportional distribution of the recovered core material over the whole respective core length. For comparison, the theoretical inclination value to be expected at the drill site has been included (dashed vertical line in the stable magnetic inclination field). The dashed vertical line in the Curie temperature field represents the Curie temperature of the unaltered, primary magnetic mineral component.*

from samples from the middle cores of Hole 427, the titanomagnetite grains always look homogeneous under the microscope.

Iron sulfides also are commonly present, often as perfect spherules, but their volume content is on the average only 0.1 per cent. In a few of the coarser grained samples, primary ilmenite could be identified (Sample 422-9-5, 72-75 cm) forming separate laths. In the center part of the thick flow in Hole 427 ilmenite occurs as secondary mineral produced by high-temperature oxidation of titanomagnetite, forming the typical ilmenite "exsolution" lamellae along the (111) planes
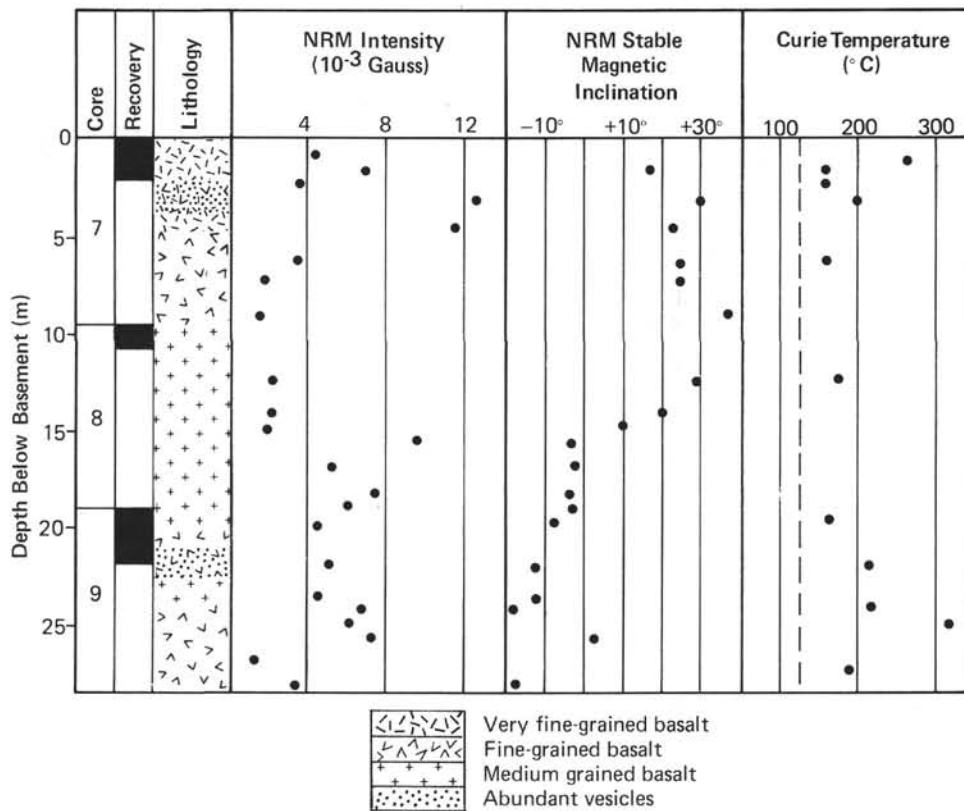
Figure 5. *Downhole plot of NRM intensity and direction and of Curie temperature for the Galapagos Hole 425. The dashed vertical line in the Curie temperature field represents the Curie temperature of the unaltered, primary magnetic mineral component.*

of the host titanomagnetite (Sample 427-10-4, 53-55 cm). Chromium spinel occurs in Sample 422-9-4, 135-138 cm.

b) Microprobe Studies and the Primary Composition of the Titanomagnetites

The deep ocean environment causes alteration of the basaltic basement. This process affects the titanomagnetites contained in the ocean-floor basalts, which consequently influences the magnetic properties of these rocks.

The dominant form of alteration of the titanomagnetites under sub-oceanic conditions is a low-temperature oxidation; this transforms the originally stoichiometric titanomagnetites into cation-deficient spinels, the so-called titanomaghemites. The process causes an increase of the Curie temperature which is roughly proportional to the degree of oxidation (Readman and O'Reilly 1972). The Curie temperature can therefore be used conveniently as a measure of the titanomagnetite submarine oxidation.

Table 3 lists the results of the microprobe studies. For the purpose of determining the primary composition of the titanomagnetites analyzed (i.e., the titanomagnetite composition prior to any alteration), one should consider the Fe migration associated with submarine titanomagnetite oxidation (Johnson and Melson 1978, Peter-

sen et al., 1979). Such Fe migration changes the original Fe/Ti ratio. This effect can be accounted for by plotting the composition against the Curie temperature as shown in Figures 6 and 7. Here the analyses of the Hole 428A samples are plotted together with other titanomagnetite analyses of oceanic tholeiites from widely different sites from the Atlantic Ocean and the Mediterranean Sea. The Hole 428A samples fall well into the general trend. From this trend a primary titanomagnetite composition of

$$Fe_{2.27}Ti_{0.58}Al_{0.07}Mg_{0.06}Mn_{0.02}O_4$$
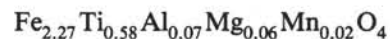
is deduced.

c) Variation of Curie Temperature with Age

Given a certain grain size of the titanomagnetites in submarine basalt, the degree of low-temperature oxidation increases with the age of the rock. Ozima et al. (1974) assumed a first-order rate process of the following form

$$z = 1 - e^{-t/\tau}$$

where z denotes the titanomagnetite oxidation parameter (O'Reilly and Banerjee 1966), t the age of the rock, and τ the time constant of the process. From their data they derived a time constant of $\tau = 5 \times 10^7$ y. On the other hand, Petersen et al. (1979) derived a logarithmic

TABLE 3
Microprobe Analyses of Titanomagnetites

Sample Hole-Core-Section, Interval in cm, Piece No.	Fe (Wt. %)	Ti (Wt. %)	Al (Wt. %)	Mg (Wt. %)	Mn (Wt. %)	Cr (Wt. %)	Total	Relative Atomic %[a]	$\dfrac{Fe}{Ti+Al+Mg+Mn}$
428A-5-2, 85-88, 5D	55.85	12.52	0.91	0.63	0.51	0.03	70.45	98.8	3.83
428A-5-2, 114-117, 6A	54.87	12.81	0.96	0.60	0.64	0.03	69.91	98.3	3.66
428A-5-4, 89-92, 6	55.73	13.92	1.02	0.65	0.74	0.04	72.10	101.6	3.41
428A-7-2, 87-89, 6	55.49	12.98	1.30	0.74	0.42	0.03	70.96	100.4	3.59
429A-3-1, 112-115, 6	54.76	12.85	1.07	0.74	0.46	0.02	69.90	98.6	3.62

[a]Atomic percentage with respect to the total cations of the stoichiometric titanomagnetite $Fe_{2.27}Ti_{0.58}Al_{0.07}Mg_{0.06}Mn_{0.02}O_4$. It gives a measure of the degree of cation deficiency in the respective spinel (Petersen et al., 1979).
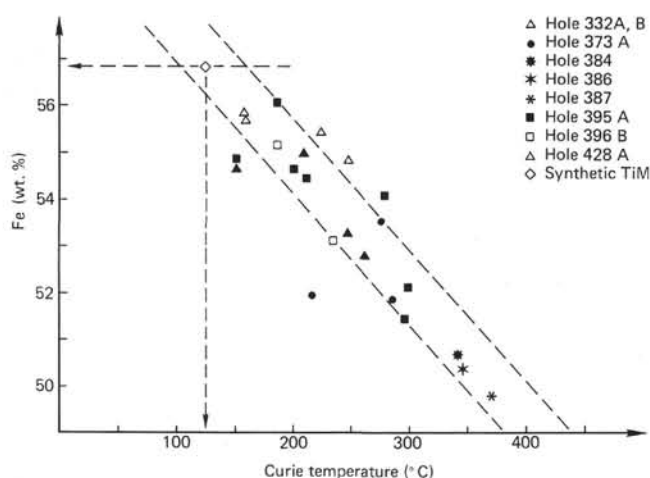

Figure 6. *Microprobe analyses of titanomagnetites contained in ocean-floor tholeiites plotted against Curie temperature, T_c. The Curie temperature indicates the degree of low-temperature oxidation of the titanomagnetites: The higher the T_c, the higher the oxidation state. A distinct iron depletion with increasing oxidation is observed. Also indicated in this diagram are the composition and Curie temperature of a synthetic spinel with a composition equivalent to the primary titanomagnetite composition as deduced from the microprobe analyses.*

Figure 7. *Microprobe analyses of titanomagnetites contained in ocean-floor tholeiites. A distinct variation of the cation ratio with low-temperature oxidation is observed. As in Figure 3 the synthetic equivalent of the primary titanomagnetite composition is also indicated. The lower dashed line represents the minimum value of the $Fe/(Ti + Al + Mg + Mn)$ ratio to be expected according to the model of Fe-migration (Petersen et al., 1979) when complete oxidation is reached.*

relationship between Curie temperature and the age of the rock.

In Figure 8, the Curie temperatures of the investigated Leg 54 basalts are plotted against their age. We observe a distinct increase of T_c with age (See also Table 4). However, the scatter of samples from a single drill hole is considerable. The most important causative factor is probably the grain size (Petersen et al., 1979). Nevertheless, it seems that such factors average out if the number of samples for a certain site is large enough. It is therefore justified to use the mean values of the Curie temperatures of the different sites, provided the number of samples is sufficiently large. If we assume an age of 3.4 m.y. for Hole 427, it clearly falls off the general trend. However, as already pointed out, this age is very uncertain. From Figure 6, an age of only 2 m.y. seems to be much more likely for this site.
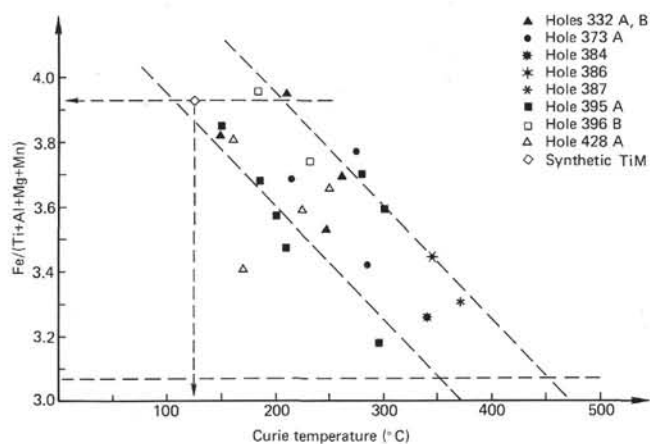
It is further interesting to note that the samples from the Galapagos geothermal area behave exactly like those from the other sites. This means that the titanomagnetite oxidation rate has not been accelerated by any abnormal circumstances like elevated temperatures or hydrothermal solutions. In Table 4, the Curie temperatures, T_c, are converted to titanomagnetite oxidation parameter z-values, using the relationship given by Petersen et al. (1979). z has been defined by O'Reilly and Banerjee (1966) as the fraction of the initial Fe^{+2} in the titanomagnetite converted to Fe^{+3}. Unoxidized titanomagnetite is characterized by $z = 0$, and completely oxidized titanomagnetite by $z = 1$. Figure 9 shows a plot of z versus the age of the rock. Data from ocean-floor basalts from the Atlantic Ocean and the Mediterranean Sea have been included in this graph. The result clearly differs from the relationship given by Ozima et al. (1974) and also from the logarithmic relationship of Petersen et al. (1979). Instead, we observe
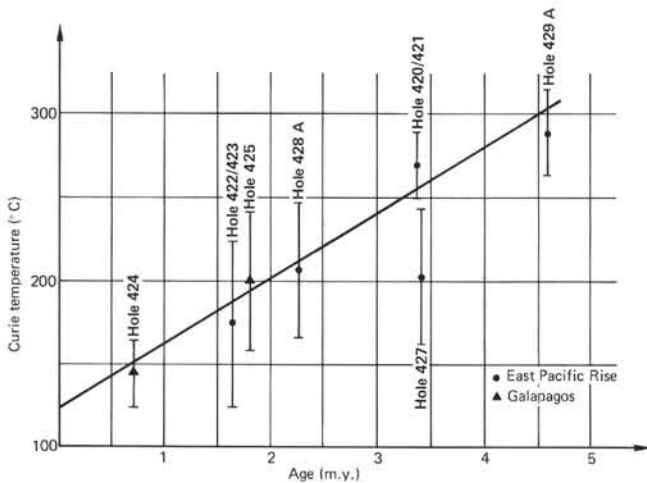
Figure 8. *Curie temperature, T$_c$, versus age of ocean floor basalts from the different Leg 54 sites.*

Figure 9. *Mean values of titanomagnetite oxidation parameter, z, plotted against the ages of the rocks. Data from ocean-floor basalts from the Atlantic Ocean and the Mediterranean Sea have been included in this graph.*

TABLE 4

Mean Values of Curie Temperature, T_C; Saturation Magnetization at Room Temperature, I_S; and Titanomagnetite Oxidation Parameter, z, for the Different Leg 54 Holes

Hole	T_C (°C)	I_S (10^{-2} Gauss cm/g)	Age (m.y.)	z
East Pacific Rise				
420	268 ± 20	16 ± 1	3.4	0.65
421	269 ± 19	11 ± 5	3.4	0.65
420+421	268 ± 20	13 ± 4	3.4	0.65
423	246 ± 8	9 ± 1	1.5	0.59
422	157 ± 46	70 ± 7	1.7	0.23
422+423	173 ± 55	59 ± 25	1.6	0.32
427	201 ± 44	148 ± 9	3.4?	0.44
428	161 ± 11	103	2.25	0.25
428A	210 ± 44	107 ± 21	2.25	0.47
428+428A	204 ± 44	106 ± 21	2.25	0.45
429A	286 ± 26	13 ±	4.6	0.69
Galapagos Spreading Center				
424A,B,C	143 ± 24	125 ± 18	0.68	0.14
425	201 ± 65	102 ± 1	1.8	0.44

two linear regions with a distinct change of slope at about 3.5 m.y.

Between 0 and 3.5 m.y., the slope $z/time$ = 0.2 y; between 3.5 and 20 m.y., $z/time$ = 0.009/y. The latter value is much less well defined.

If the relationship of Figure 9 were valid for the oceanic basement in general, it would mean that about two thirds of the titanomagnetite oxidation takes place within the first 3.5 m.y., and the rest at a much slower rate over a very long period.

This may be an important factor for the formation of iron deposits along active spreading centers. According to Johnson and Melson (1978) and Petersen et al. (1979), submarine titanomagnetite low-temperature oxidation involves the release from the spinel crystals of an amount of Fe which is proportional to z. Consequently, two thirds of the iron that can be mobilized from the titanomagnetites by this process is released within a nar-
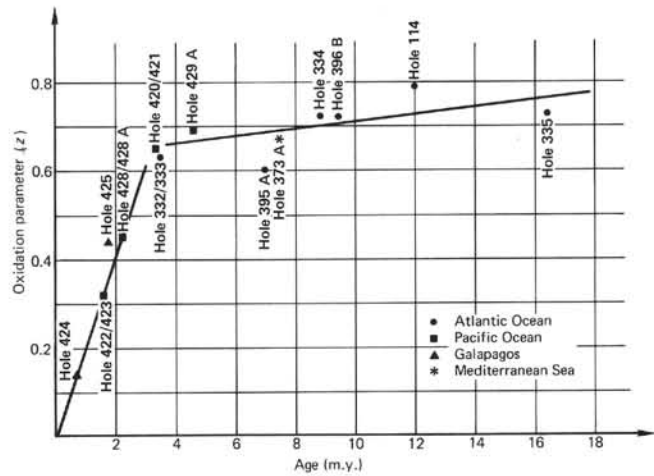
row band along the spreading axis of only 3.5 m.y., corresponding to 35 km for a spreading rate of 1 cm/y.

d) Susceptibilities

Most of the susceptibilities of the basalts are high in comparison to basalts from Leg 37. Similarly, the median destructive fields are also typically low (less than 100 Oe). The relationship between MDF and susceptibility is shown in Figure 10.

Most samples recovered from both PAC-4 and the Galapagos areas plot in the lower right-hand corner. Exceptions to this are very fine grained basalts from Hole 422 with very high MDF's and correspondingly low susceptibilities. Also shown in this diagram are samples recovered from Leg 41. Most samples from Leg 37 plot further to the upper left of the figure; however, a few exceptions do fall in the upper limits of the Leg 54 samples. The seven Leg 41 basalts have high susceptibilities and low MDF's but still fall along a trend established by the Leg 37 and Leg 54 basalts.

There are two explanations for the trend displayed by these data. First of all, an inverse relationship exists between MDF and susceptibility such that MDF decreases as susceptibility increases (Stacey and Banerjee, 1974). Consequently, the data may be interpreted to represent changing physical parameters, such as grain size, in a unimodal iron oxide system. Alternatively, it is possible to regard deep-sea basalts as a bimodal or multimodal mixture of grain sizes. The larger grains contribute most heavily to the susceptibility, since they would be primarily multi-domained and hence easily affected by imposed magnetic fields. The smaller grains have low susceptibilities but high magnetic stabilities. Therefore, in the diagram presented, samples plotting in the lower right would be dominated by large grains, whereas those with higher MDF's are dominated by the finer grains.
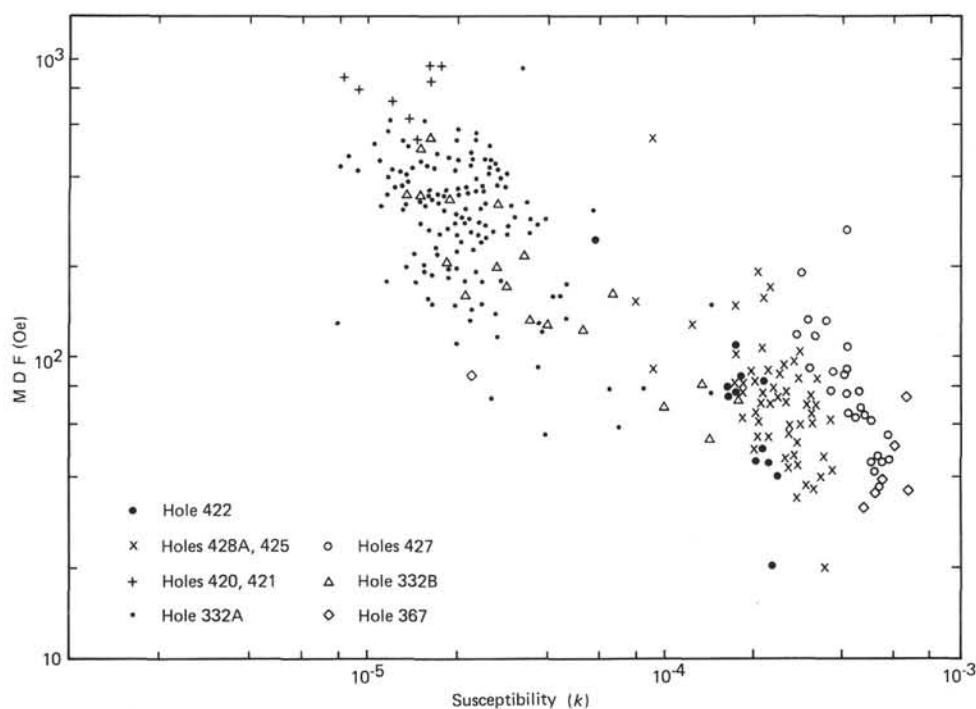
Figure 10. *Susceptibility of oceanic basalts plotted against median destructive field (MDF). Data from Hole 332A are from Hall and Ryall (1977) and Bleil and Petersen (1977). Data from Hole 332B are from Bleil and Petersen (1977). The data from Hole 367 are taken from Kent and Tsai (1978).*

Between the two large groups of data an area of relatively few data points exists. This barren zone may simply be the result of an insufficient sample population, especially since samples from Hole 321 seem to show a tendency to bridge the gap. More likely, this gap may be real and may relate to processes occurring during cooling and alterations.

Fine-scale trends also exist within the general grouping. For example, Site 427 rocks show a well-defined trend along the upper edge of the main body of the low MDF data grouping. Site 422 rocks made a similar trend along the bottom edge of that grouping. The individual trends of these data are comparable but have higher slope than the overall band of data. This larger slope may be due to the acquisition of remanence during drilling. The artificial remanence would have the effect of apparently reducing the MDF because the drilling remanence is easily removed.

SUMMARY AND CONCLUSIONS

1) Both sampling areas were too close to the equator to permit a correlation between the polarity of the remanent magnetization of the drilled samples and the sign of the overlying marine magnetic anomaly. This is because only the inclination of the remanent magnetization of the drill core can be determined absolutely. At the latitude of the EPR sampling area the theoretical inclination of an Earth-centered dipole field is 18°. This value can be exceeded easily by the secular variation of the Earth's magnetic field.

2) In Hole 425, situated at about 1° N, a downhole variation of the inclination values of the remanent magnetization of 40° has been determined. We interpret this variation as being due mainly to the secular variation of the Earth's magnetic field at this site. Tilting may also contribute to this value.

3) In agreement with earlier studies it has been found that the NRM of the basalts is carried by small grains of titanomagnetites with an average volume content of 1 per cent in the fragmented rocks of Holes 420, 421, 422, 423, 429A, and of about 3 per cent in the coarser grained rocks of Holes 427 and 428A. Skeletal titanomagnetite grains are typical in all samples.

4) The titanomagnetites are oxidized gradually under sub-oceanic conditions and form thereby cation-deficient spinels, the so-called titanomaghemites. This oxidation proceeds at low temperatures, most likely at ocean-floor water temperature.

5) The primary composition of oceanic titanomagnetites varies only within narrow limits. The samples studied in this paper group well around a composition of

$$Fe_{2.27}Ti_{0.58}Al_{0.07}Mg_{0.06}Mn_{0.02}O_4.$$
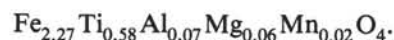
6) The Curie temperature, T_c, of the basalts investigated increases with age of the oceanic crust. T_c can be converted to the oxidation parameter, z, of the titanomagnetites. When z is plotted against the age of the rock, two linear segments are obtained with a change in the slope at an age of 3.5 m.y. Between an age of 0 and

3.5 m.y. the slope $z/time = 0.2$ m.y.; and between 3.5 and 20 m.y., $z/time = 0.009/y$.

7) The high rate of titanomagnetite sub-oceanic oxidation in the first 3.5 m.y. may be an important factor for the formation of iron deposits along active spreading centers.

8) From the relationship of z with age, an age of about 2 m.y. is deduced for Site 427.

9) The susceptibilities and MDF's form an interesting pattern when combined with data from Leg 37 and Leg 41 basalts. The grouping of data into semi-discrete regions suggests that this type of diagram would be very helpful in distinguishing between basalt populations.

ACKNOWLEDGMENTS

REFERENCES

Bleil, U. and Petersen, N., 1977. Magnetic properties of basement rocks, Leg 37, Site 332. *In* Aumento, F., Melson, W. G., et al., *Initial Reports of the Deep Sea Drilling Project,* v. 37: Washington (U. S. Government Printing Office), p. 449–456.

Grommé, C. S., Wright, T. L., and Peck, D. L., 1969. Magnetic properties and oxidation of iron-titanium oxide minerals in Alae and Makaopuhi lava lakes, Hawaii. *J. Geophys. Res.,* v. 74, p. 5277–5293.

Hall, J. M. and Ryall, P. J. C., 1977. Paleomagnetism of basement rocks, Leg 37. *In* Aumento, F., Melson, W. G., et al., *Initial Reports of the Deep Sea Drilling Project,* v. 37: Washington (U. S. Government Printing Office), p. 425–448.

Johnson, H. P. and Hall, J. M., 1978. A detailed rock magnetic and opaque mineralogy study of the basalts from Nazca plate. *Geophys. J. Roy. Astr. Soc.,* v. 52, p. 45–64.

Johnson, H. P. and Melson, W. G., 1978. Electron microprobe analyses of some titanomagnetite grains from Hole 395A. *In* Melson, W. G., Rabinowitz, P. D., et al., *Initial Reports of the Deep Sea Drilling Project,* v. 45: Washington (U. S. Government Printing Office), p. 575–579.

Kent, D. V. and Tsai, L. P., 1978. Paleomagnetism and rock magnetism of Upper Jurassic limestone and basalt from Site 367. *In Initial Reports of the Deep Sea Drilling Project, Supplement to volumes 38, 39, 40, and 41:* Washington (U. S. Government Printing Office), p. 995–1002.

LaBrecque, J. L., Kent, D. V., and Cande, S. C., 1977. Revised magnetic polarity time scale for Late Cretaceous and Cenozoic time. *Geol.,* v. 5, p. 330–335.

Maniken, E. A. and Dalrymple, G. B., 1979. Revised geomagnetic polarity time scale for the interval 0-5 m.y. B.P. *J. Geophys. Res.,* v. 84, p. 615–626.

O'Reilly, W. and Banerjee, S. K., 1966. Oxidation of titanomagnetites and self-reversal. *Nature,* v. 221, p. 26–28.

Ozima, M., Joshida, M., and Kinoshita, H., 1974. Magnetic properties of submarine basalts and the implications on the structure of the ocean crust. *J. Geomag. Geoelectr.,* v. 26, p. 335–354.

Petersen, N., Eisenach, P., and Bleil, U., in press. Low temperature alteration of the magnetic minerals in ocean floor basalts. *Maurice Ewing Series,* v. 1, Washington (American Geophysical Union).

Prévot, M. and Lacaille, A., 1976. Sur le charactere episodique du fonctionnement des zones d'accretion: critique des arguments geomagnetiques. *Bull. Soc. Geol. France,* (7), v. 18, p. 903–911.

Readman, P. W. and O'Reilly, W., 1972. Magnetic properties of oxidized (cation-deficient) titanomagnetites (Fe, Ti)$_3$O$_4$. *J. Geomag. Geoelectr.* v. 24, p. 69–90.

Sclater, J. G. and Klitgord, K. D., 1973. A detailed heat flow, topographic, and magnetic survey across the Galapagos Spreading Center at 86°W., *J. Geophys. Res.,* v. 78, p. 6951–6975.

Stacey, F. D., and Banerjee, S. K., 1974. *The Physical Principles of Rock Magnetism*: Amsterdam, London, New York (Elsevier Scientific Publishing Company).